JOURNAL OF CATALYSIS 136, 283–299 (1992)

Single-File Diffusion and Reaction in Zeolites

JÖRG KÄRGER,* MICHAEL PETZOLD,* HARRY PFEIFER,* STEFAN ERNST,† AND JENS WEITKAMP†

*Department of Physics, University of Leipzig, Linnéstrasse 5, D-O-7010, Leipzig, Germany; and †Institute of Chemical Technology I, University of Stuttgart, Pfaffenwaldring 55, D-W-7000 Stuttgart 80, Germany

Received July 30, 1991; revised February 15, 1992

Mass transfer and chemical reaction in channels in which the individual molecules cannot pass each other (single-file systems) are studied by Monte Carlo simulations. Applying a simple jump model for the elementary steps of diffusion, macroscopically observable phenomena like molecular adsorption and desorption, tracer exchange, and counterdiffusion are considered. In the case of chemical reaction, the simulation results are used for a generalization of the Thiele concept to single-file systems. © 1992 Academic Press, Inc.

INTRODUCTION

In the past decade, the development of zeolite research and technology has been intimately connected with the tremendous achievements in the synthesis of new zeolite structures (*1–4*). Among these, the great variety of zeolites with one-dimensional channel systems (e.g., ZSM-12, -22, -23, -48, $AlPO_4$-5, -8, -11, L, Omega, EU-1, and VPI-5) deserves special attention from both a theoretical and a practical point of view. As soon as the diameters of the molecules migrating within such adsorbents are comparable with the diameters of the channels, the individual molecules cannot pass each other within a channel. This situation may be compared with a file of strung pearls, where a given pearl may only be shifted if the adjacent ones are shifted as well, in order to leave the necessary free space for displacement. It is obvious that molecular transportation under such conditions is quite different from "ordinary" diffusion, where the molecules may exchange their positions. Referring to the similarity with conductance mechanisms in biological membranes (*5, 6*), Riekert (*7*) was probably the first to apply this concept of *single-file diffusion* to molecular migration in zeolites. With the advent of the broad variety of microporous materials in which single-file diffusion can occur, Riekert's pioneering work (*7*), which appeared more than 20 years ago, has gained particular importance. Apart from the developments in zeolite research as an example for correlated processes in multiparticle systems, single-file diffusion has become an attractive topic for mathematicians and theoretical physicists. As the most important result, for sufficiently long observation times t the mean square displacement $\langle r^2(t)\rangle$ of the individual particles in file direction was found to be proportional to the square root of the observation time. This is in contrast to ordinary diffusion, where, according to Einstein's relation

$$\langle r^2(t)\rangle = 2Dt, \tag{1}$$

the mean square displacement is proportional to the observation time with D denoting the self-diffusivity. Assuming that molecular diffusion proceeds via activated jumps with step length l and a mean time τ between succeeding jumps, the self-diffusivity is related to the elementary steps by

$$D = \frac{l^2}{2\tau}. \tag{2}$$

As a long-time approximation for the

0021-9517/92 $5.00

mean square displacement for single-file diffusion, Fedders (*8*) derived the following analytical expression:

$$\langle r^2(t)\rangle = l^2 \frac{1-\Theta}{\Theta}\sqrt{\frac{2}{\pi}}\sqrt{\frac{t}{\tau}}. \qquad (3)$$

The meaning of the quantities l and τ is in analogy to Eq. (2), but with the understanding that now one must consider jump attempts rather than real jumps and that a jump attempt is only successful if it is directed to a vacant site. Θ denotes the fraction of occupied sites. The step length coincides with the separation of adjacent sites. The derivation of Eq. (3) as presented in Ref. (*8*) is based on the formalism of the two-point correlation function and requires a substantial theoretical background (see, e.g., (*9*)). However, Eq. (3) may be derived in a much easier way by simply considering the random walk of the involved vacancies. This derivation, which is in fact an extension of de Gennes' treatment of polymer "reptation" (*10*), is given in the Appendix.

Adopting the notation of Einstein's relation (Eq. (1)) it may be appropriate to introduce a single-file mobility factor F by the equation

$$\langle r^2(t)\rangle = 2F\sqrt{t} \qquad (4)$$

with the dimension $m^2\,s^{-1/2}$. Using Fedders' approximation (Eq. (3)) one has

$$F = l^2 \frac{1-\Theta}{\Theta}\frac{1}{\sqrt{2\pi\tau}}. \qquad (5)$$

For interpreting experimental data it may be useful to introduce a "concentration-corrected" single-file mobility factor F_0 by incorporating the explicit concentration dependence given by Eq. (5):

$$F_0 = F\frac{\Theta}{1-\Theta} = \frac{l^2}{\sqrt{2\pi\tau}}. \qquad (6)$$

Being not explicitly dependent on concentration, Eq. (6) can be considered as the single-file counterpart of Eq. (2).

The different time dependence of the mean square displacements in ordinary and single-file diffusion results from the difference in the correlation of molecular displacements in subsequent time intervals (*11*). In the case of ordinary diffusion, considering sufficiently large time intervals, these displacements are completely uncorrelated. This leads to the well-known behavior of Markoffian processes in which the distribution width of the square displacements increases in proportion to the considered time. One may easily rationalize this fact by summing up the displacements in succeeding time intervals and taking the mean square of the sum. Due to the loss of coherence in different time intervals, all cross terms vanish and one obtains the sum of the square displacements during the individual intervals, i.e., a quantity that is proportional to the number of succeeding time intervals and with it to the time itself. In single-file diffusion, a displaced molecule is more likely to return to its original position than to proceed further, since the latter would stipulate a further concentration of the molecules ahead. Consequently, molecular displacements in succeeding time intervals are more likely to occur in opposite directions, leading to negative cross terms in the mean square sum of the displacements. It is essential that this correlation is preserved for any time interval and that it is more stringent the larger the considered displacements. Thus one may easily rationalize the fact that the mean square displacement increases less than linearly with the observation time. It should be emphasized that negative cross terms between succeeding displacements may occur for a variety of diffusion mechanisms as soon as a mutual interaction of the diffusants becomes essential. This is described by the well-known correlation effect (*12*), leading to diffusivities smaller than expected from the elementary steps on the basis of a pure random model as provided by Eq. (2). However, for other than single-file systems this correlation vanishes with increasing time intervals, (*13*), and for observation times sufficiently

surpassing the time scale of the elementary steps, molecular migration follows Einstein's equation (Eq. (1)) of ordinary diffusion. This fact has been confirmed experimentally for self-diffusion in both solids (*12*) and zeolitic adsorbate–adsorbent systems with three-dimensional pore networks (*14*); it should be worthwhile, therefore, to reserve the term single-file diffusion for real single-file systems as introduced above.

Since the pioneering publications of Ruthven (*15*) and Theodorou and Wei (*16*), Monte Carlo simulations of molecular mass transfer have become routine methods in zeolite research (*17–22*). So far, however, one was in general concerned with more-dimensional networks. To our knowledge, only Rajadhyaksha and co-workers (*20–22*) have considered a situation similar to the above described case of single-file diffusion. However, they have not explored the long-time dependence in any detail. In their representations the mean square displacements appear to approach a constant value, which would be in contrast to the behavior predicted in theory.

It is clear that one-dimensional diffusion in channel-like pores does not necessarily imply single-file behavior. As soon as the individual molecules may pass each other, ordinary diffusion may become dominant. Depending on the ease of this mutual passage and the location where it may occur (i.e., anywhere in the channel system, in side pockets, or in structural defects), there might be a broad transition range between these two diffusion regimes. Moreover, since different experimental techniques may differ in both the observable displacements and time scales (*23, 24*), it may be possible that in experiments carried out with different methods, different diffusion mechanisms prevail.

In the present paper, the method of Monte Carlo simulation is applied to predict some of the key features of molecular migration and reaction under the conditions of single-file diffusion.

THE MOLECULAR MEAN SQUARE DISPLACEMENT

The single-file system is assumed to consist of a chain of N sites of separation l, and $z = N\Theta$ molecules are statistically distributed over the sites. Molecular transport within this system is simulated by repeating the following operations:

(i) statistical selection of one of the z molecules for a jump attempt (activation),

(ii) statistical selection of the jump direction,

(iii) the molecule jumps to the adjacent site if it is vacant, otherwise it remains at its position.

z activations are considered as one step in the simulation procedure. With τ denoting the mean jump time (i.e., the mean time between two succeeding activations of the same molecule), the number of simulation steps n is related to the simulated time t by $t = n\tau$. To reduce the influence of disturbing boundary effects, the considered finite file is periodically prolonged in either direction; i.e., the rightmost molecule of the chain can only jump to the right, if the leftmost site is vacant. The dependence of the mean square displacement, obtained in this manner, on the step number (and, hence, on the observation time) is shown in Fig. 1 for different medium occupation numbers Θ. The data represent the medium values obtained after several runs (accumulations). For smaller site occupancies, corresponding to a smaller total amount of molecules, larger accumulation numbers were chosen to keep the scattering in the obtained data at a level comparable with the one at higher occupancies. In agreement with the analytical approximation, for sufficiently large step numbers the mean square displacements increase proportionally to the square root of the observation time yielding in the logarithmic representation a straight line with slope $\frac{1}{2}$. Following the notation of Eq. (4), Fig. 2 shows values for the single-file mobility factor F as determined from the intercept of the long-time approximations of Fig. 1 with the

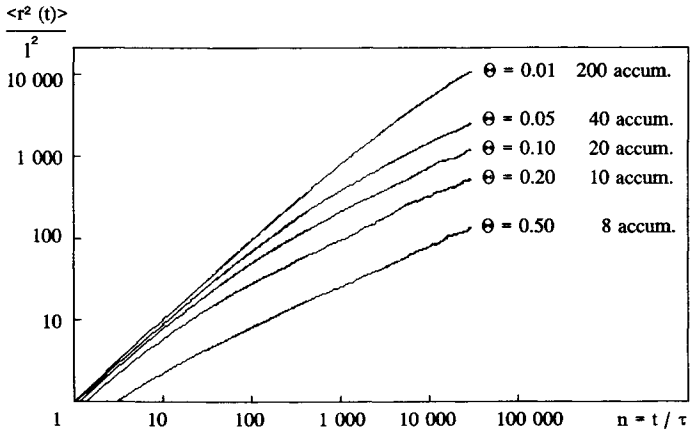

FIG. 1. Molecular mean square displacements in dependence on the observation time t on a single file of $N = 10{,}000$ sites for various site occupancies Θ. The plots represent the mean values of several simulation runs (accumulations) as indicated in the figure.

ordinate (corresponding to the slope of a $\langle r^2(t)\rangle$-vs-$t^{1/2}$ representation) and the concentration-corrected values F_0 in dependence on Θ. In agreement with Eq. (6), F_0 is found to be essentially concentration independent. In contrast to previous Monte Carlo simulations (*25*), the absolute values are as well in agreement with the theoretical prediction

$$\frac{F_0\sqrt{\tau}}{l^2} = \frac{1}{\sqrt{2\pi}} \approx 0.4 \qquad (7)$$

as given by Eq. (6).

The typical single-file behavior, i.e., proportionality between $\langle r^2(t)\rangle$ and $t^{1/2}$, is observed sooner, the closer the concentrations are to complete saturation. Vice versa, the initial regime of ordinary diffusion is best expressed for small occupation numbers. Both effects are easily understandable since it is the effect of mutual collisions that leads to the transition from ordinary to single-file diffusion, and these collisions are clearly more frequent for higher occupation numbers.

A systematic error in the determination of

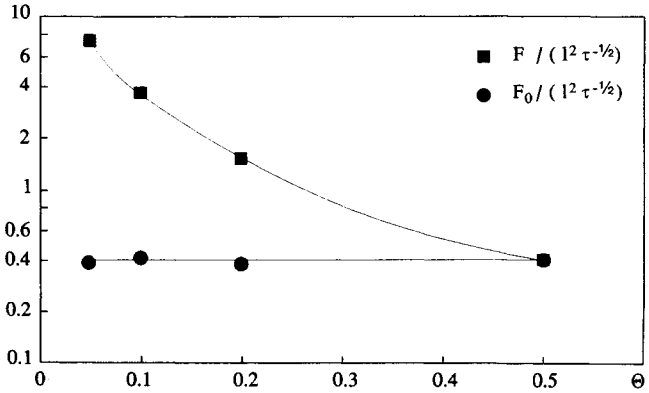

FIG. 2. Single-file mobility factor F and concentration-corrected mobility factor F_0 resulting from the Monte Carlo simulations presented in Fig. 1, in dependence of the file occupancy Θ.

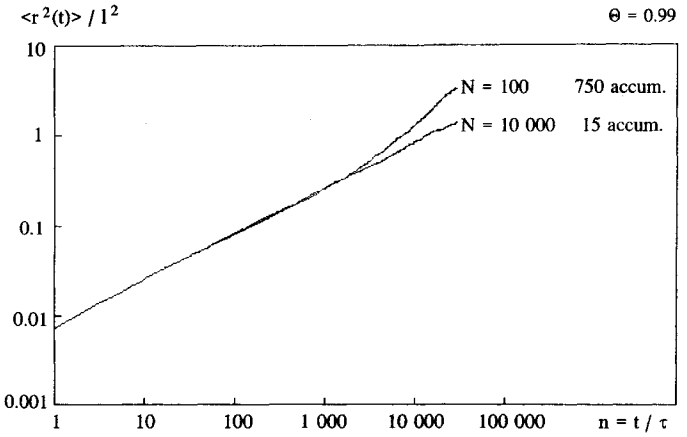

FIG. 3. Influence of the single-file chain length Nl for a correct determination of the long-time behavior of the mean square displacement.

the mean square displacements may occur if the file lengths Nl are not chosen long enough. This is illustrated by Fig. 3, where for the shorter file, starting from a certain step number ($n \approx 1000$), the time dependence of ordinary diffusion is again observed. For this comparison a very high site occupancy ($\Theta = 0.99$) was selected to ascertain that single-file behavior is obtained from the very beginning of the observation times t (see Fig. 1). The deviation from single-file behavior as observed for the shorter file is a consequence of the fact that for a "vacancy" leaving the original file, due to the used principle of periodic repetition, this vacancy and its "mirror" (starting from the other side of the file) would migrate to the file center with equal probability. This means that, notwithstanding the fact that this vacancy has shifted a given molecule to a certain direction, as soon as this vacancy has attained the boundary, on "returning" (either by itself or as its mirror) it may effect a shift of this very molecule to either side, i.e., a shift independent of the history. Thus, again Markoffian behavior leading to ordinary diffusion would be observed.

Being directly sensitive to molecular mean square displacements, pulsed field gradient (PFG) NMR spectroscopy appears to be a very appropriate tool for discriminating between ordinary and single-file diffusion (*26–28*). The prospects of the applicability of PFG NMR are improving with increasing molecular mean square displacements and molecular concentrations. For the measurement of normal diffusion in adsorbent–adsorbate systems, these conditions are often found to be contradictory (concentration dependences of type I, II, or IV (*23, 26*) exhibiting decreasing diffusivities with increasing concentrations). The concentration dependence of the mean square displacements as given by Eqs. (4) and (5) indicates that this is also true for single-file diffusion. To obtain an idea of the range of relevant root mean square displacements in single-file diffusion one may estimate the quantity τ in Eq. (3) on the basis of Eq. (2). Figure 4 presents the observation times necessary for following certain single-file mean diffusion paths $\langle r^2(t)\rangle^{1/2}$ calculated in this way for a step length of 5 Å and a diffusivity of 10^{-8} m^2 s^{-1}. The latter value is of the order of the diffusivity determined by both PFG NMR measurements (*29*) and Molecular Dynamics calculations (*30, 31*) for methane in the channel network of zeolite ZSM-5 and is probably a reasonable upper limit for sorbate diffusivities in zeolites. Realizing that a value of 0.1 ... 1 μm is a

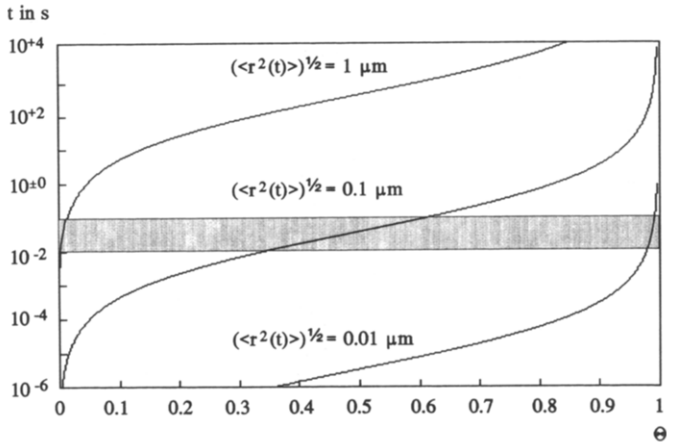

FIG. 4. Observation times t necessary for following various single-file mean diffusion paths $\langle r^2(t)\rangle^{1/2}$ in dependence on the site occupancy Θ, calculated from Eqs. (2) and (3) with $D = 10^{-8}\ m^2\ s^{-1}$ and $l = 5$ Å. The shaded area represents the region of maximum observation times accessible by PFG NMR.

typical lower limit for the range of displacements presently accessible by PFG NMR (*27*), and since, on the other hand, the maximum observation times in PFG NMR studies with zeolites are of the order of 10 ... 100 ms, this representation illustrates that only for relatively small site occupancies contributions of PFG NMR studies to the understanding of single-file diffusion in zeolites may be expected.

The measuring range of quasi-elastic neutron scattering as an alternative method for studying intrinsic diffusion phenomena (*32*) comprises the other extreme case of displacements in the nanometer range. Such measurements are therefore particularly useful for high concentrations.

THE SINGLE-FILE ADSORPTION ISOTHERM

In view of the above described limitations to the microscopic measuring techniques of single-file diffusion, the macroscopic description of the single-file behavior of adsorbate–adsorbent systems, i.e., the prediction of the response of the whole system to a change in the concentration or composition of the surrounding atmosphere, has special relevance. Maintaining the procedure of the previous section for simulating intracrystalline single-file diffusion, molecular exchange between the crystallites and the gas phase is considered in the following way:

(i) If the incidentally selected molecule occupies the last site of the file and if the jump attempt is directed out of the file, the molecule may leave the file with the probability P; otherwise it remains at its position.

(ii) During each simulation step (i.e., per z jump attempts of the molecules within the file) on either side of the single file, a molecule from outside the file tries q times to occupy the last file position. It is successful if the position is vacant.

Translated to real physical quantities, the encounter rate q at the channel orifice is a measure of the gas-phase pressure. The escape probability P is related to the adsorption energy E by the Boltzmann relation

$$P \propto e^{-E/k_bT} \tag{8}$$

indicating the probability that a particle is able to overcome a step E in the potential energy. With the boundary conditions modi-

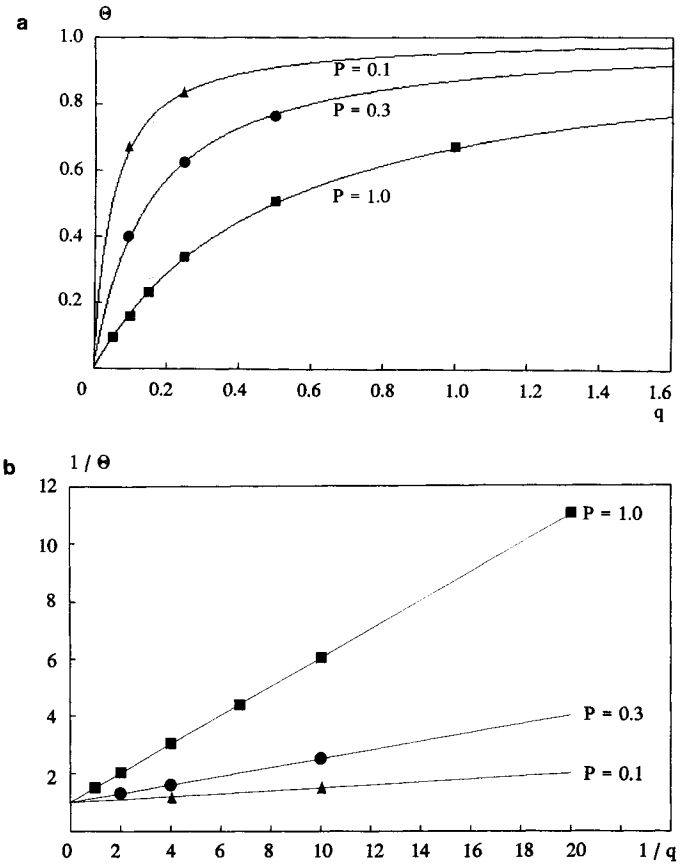

FIG. 5. Equilibrium single-file site occupancy Θ in dependence on the encounter rate q of molecules from the gas phase for various escape probabilities P (a) and Langmuir-type representation of the resulting relation (b). q is represented in molecules per orifice and simulation step and is proportional to the external pressure of the gas.

fied in this manner, starting from zero concentration, the above described simulation of intracrystalline single-file diffusion has been repeated. Figure 5a shows the equilibrium concentration Θ obtained in this way after a sufficiently large number of simulation steps in dependence on the encounter rate q (and with it on the gas-phase pressure) for three different values of the escape probability P.

These curves represent nothing other than the adsorption isotherm of the single-file system. In Fig. 5b, $1/\Theta$ is plotted as a function of $1/q$ showing the typical Langmuir-type behavior

$$\frac{1}{\Theta} = 1 + \frac{1}{Kq} \tag{9}$$

of localized adsorption (*7, 33*), where the parameter K (representing the Henry constant of the simulated adsorption isotherm) is found to be related to the escape probability by

$$K = \frac{2}{P}. \tag{10}$$

This is the relation that results from a simple consideration of the conditions for dynamic equilibrium between the marginal file sites and the gas phase. The coincidence

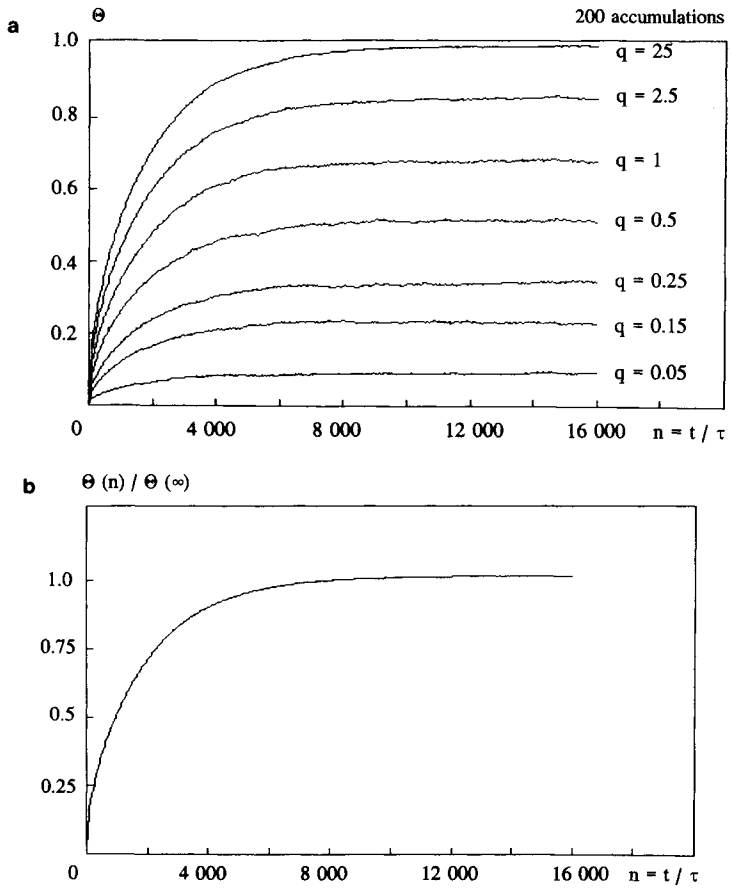

FIG. 6. Simulated curves of single-file uptake from zero concentration up to various final site occupancies corresponding to the given external pressure p, which is proportional to the quantity q, for $P = 1$ and $N = 100$. (a) Uptake in relative site occupancies. (b) Uptake in fractions of the final site occupancy.

is not unexpected since the microdynamic constraint of the individual molecules should not affect their equilibrium behavior. In agreement with this consideration, the equilibrium concentrations were found to be independent of the file length.

MOLECULAR UPTAKE

Figure 6a shows the uptake curves simulated as described above from zero up to equilibrium concentration for seven different "pressures." A plot of the fractional uptake $(\Theta(n)/\Theta(\infty))$ in Fig. 6b leads to a unique curve which, moreover, is found to coincide with the relation

$$\frac{\Theta(t = n\tau)}{\Theta(\infty)} = 1 - \frac{8}{\pi^2}\sum_{i=0}^{\infty}\frac{1}{(2i+1)^2}e^{-(D(2i+1)^2\pi^2 t/L^2)} \quad (11)$$

for molecular uptake by ordinary, one-dimensional diffusion (*23, 33*) with a diffusivity D given by Eq. (2) and $L = Nl$ as the length of the file. At first glance, it may be surprising that uptake on a single-file system should proceed as fast as under the conditions of ordinary diffusion where molecules may exchange their positions. However, if one bears in mind that a mutual exchange of two molecules in no way changes the

macroscopically observable situation, this result appears to be quite reasonable. In agreement with this consideration a dependence as predicted by Eq. (11) was also simulated (*34*)

(i) for the fractional uptake for initial concentrations different from zero,
(ii) for desorption instead of adsorption, and
(iii) for varying file lengths.

Single-file desorption was simulated by reducing rather than increasing the encounter rate q. In this way it is realized that the molecular escape rate (being equal to the encounter rate under equilibrium conditions) exceeds the encounter rate. The net effect of this difference appears as the macroscopically observable phenomenon of desorption. For computational convenience all adsorption and desorption curves have been simulated under the assumption that the escape probability P from the marginal sites is equal to one. It is essential to note that a reduction of P (i.e., an enlargement of the potential step that the molecules must overcome on leaving the file) in no way changes the desorption kinetics, as long as the file is long enough, i.e., as long as the mean time to overcome this step is much smaller than the mean travelling time from a medium position of the molecule to the file boundary (*35*). It is sorption equilibrium rather than kinetics that is influenced by the escape parameter. This has been confirmed in simulations with varying values of the escape parameter P. In contrast to the equilibrium values finally attained (see above), in all cases the time dependence leading to these values remained unaffected by this variation (*34*). Although, according to these considerations, single-file uptake appears to proceed at rates similar to those of molecular uptake in three-dimensional pore systems, there may be a substantial difference from a practical point of view. In single-file diffusion a blockade of pore orifices will lead to a significant reduction of the uptake rates and (in the case of total blockade) of the equilibrium concentration, since there is no other access to the individual channels. In a three-dimensional network, due to the internal interchange only an obstruction of essentially all orifices should lead to perceptible effects which in fact have been observed by NMR tracer desorption experiments (*36–38*) after a suitable zeolite modification.

TRACER EXCHANGE AND COUNTERDIFFUSION

The single file is assumed to be in equilibrium with the surrounding gas phase. At time zero a macroscopically observable exchange process is initiated by replacing the molecules in the gas phase (species A) by a different species (B). If these two species were isotopes, one would have to do with an example of single-file tracer exchange. In the case of two chemically different species, single-file counterdiffusion would be simulated. For simplicity both species are assumed to behave identically so that the patterns of tracer exchange and counterdiffusion (*39–41*) coincide. The gas reservoir and the transportation rate in the gas phase are assumed to be large enough so that also after desorption of type A molecules, only molecules of type B are captured by the adsorbent. Since the properties of the two species have been assumed to be identical, during the exchange process the total amount of adsorbed molecules does not change. Figure 7a shows the relative amount of adsorbed type B species in dependence on the step number n (observation time) for three different file lengths. The most striking feature of these dependences is the dramatic decrease of the exchange rate with increasing file lengths. Since the mean square displacements have been found to increase with the square root of the observation time, a scale invariant expression should be expected on plotting the relative exchange in dependence on the observation time (or the step number) over the fourth power of the file length. Figure 7b demonstrates that this behavior is in fact observed. The remaining differences be-

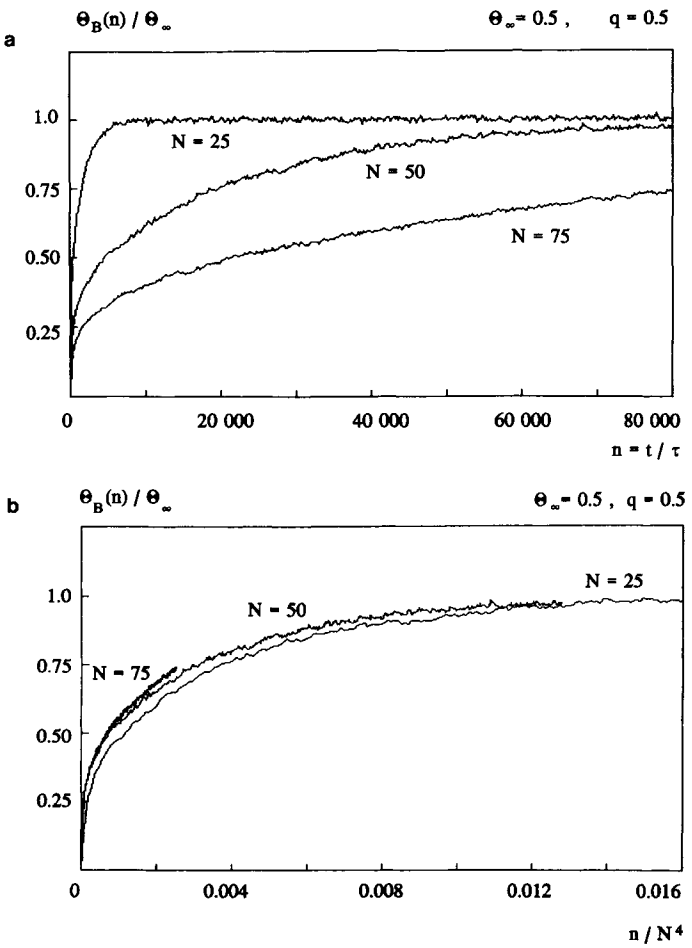

FIG. 7. Simulated curves of single-file tracer exchange (counterdiffusion) for various file lengths Nl represented in dependence on the step number (a) and the reduced step number n/N^4 (b).

tween the curves can be attributed to the fact that strict proportionality between the mean square displacement and the square root of the observation time is only attained for sufficiently large distances.

For tracer exchange under the conditions of ordinary diffusion as well as for adsorption/desorption in the cases of both normal and single-file diffusion the time constants are proportional to the square of the file length (see Eq. (11)). As a characteristic feature of tracer exchange under single-file conditions, the time constant is now found to be proportional to the fourth power of the file length.

Single-file exchange measurements will clearly require observation times much longer than those of exchange measurements in the case of ordinary diffusion. Spectroscopic methods (*37, 41, 42*) that allow tracer exchange measurements within sealed samples (which may be easily repeated over deliberately long periods) might therefore be of special relevance.

SINGLE-FILE REACTION

Within the file, a monomolecular reaction $A \rightarrow B$ is simulated by converting a statistically selected fraction κ of molecules A to B per simulation step. The quantity κ is con-

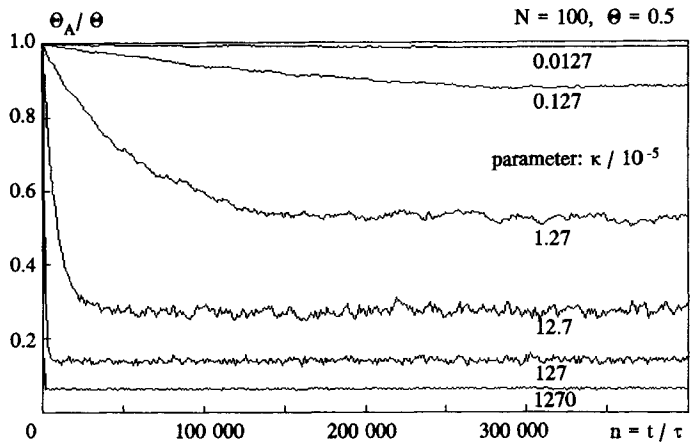

FIG. 8. Relative amount Θ_A/Θ of molecules of species A within a single file of $N = 100$ sites at a site occupancy $\Theta = 0.5$ under the conditions of chemical reaction A → B in dependence of the simulation steps n after the start of the reaction.

nected with the intrinsic reactivity k by the relation

$$k = \frac{\kappa}{\tau}. \tag{12}$$

If the selected molecules are already of type B they are left unchanged. It is assumed that in the gas phase A is in excess and that therefore only molecules of type A are captured by the marginal sites of the file.

The simulation is started with a file containing only molecules of type A in equilibrium with the surrounding gas phase. Figure 8 illustrates the conversion of these molecules to B as a consequence of the considered reaction. Depending on the given reaction rates, after a certain number of simulation steps stationary conditions are attained; i.e., the concentration of molecules of type A is not reduced any longer. Figure 9 shows the relative concentration of the molecules of type B within the single-file system in dependence of the distance from the file surface under stationary conditions for various reactivities κ.

For ordinary diffusion, the concentration profile under stationary conditions is given (*7*, *23*) by the relation

$$\frac{\Theta_B}{\Theta} = 1 - \frac{\cosh(x\sqrt{k/D})}{\cosh(L/2\sqrt{k/D})} \tag{13}$$

with x denoting the distance from the middle of the file. An example of such a concentration profile is included in Fig. 9. It illustrates that the steric confinement within the single-file system leads to an enrichment of the reaction products in the file center, which is still more pronounced than in the case of ordinary diffusion. Under stationary conditions, the effective reactivity k^* is related to the intrinsic reactivity k by the equation

$$k^* = \frac{\overline{\Theta}_A}{\Theta} k, \tag{14}$$

where Θ_A denotes the mean value of the site occupancy of molecules A. The ratio

$$\eta = \frac{k^*}{k} = \frac{\overline{\Theta}_A}{\Theta} \tag{15}$$

represents the effectiveness factor, which may be easily determined by integrating over the concentration profile. Figure 10a shows the effectiveness factors calculated in this way from the simulation results for a variety of simulation parameters.

In the Thiele concept of reaction under the conditions of ordinary diffusion, the effectiveness factor η for a parallel-sided slab of catalyst of thickness L is found to be a function of a single parameter, the Thiele modulus

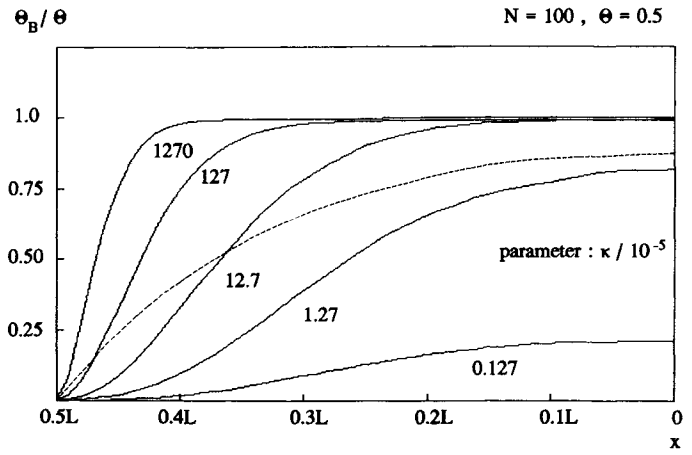

FIG. 9. Concentration profiles of the molecules of species B within the single-file system under stationary conditions and comparison with the dependence to be expected for ordinary diffusion (broken line, Eq. (13)). The quantity $2L(k/D)^{1/2}$ (the Thiele modulus Φ) in Eq. (13) has been chosen to coincide with the generalized Thiele modulus (cf. Eq. (20)) of the single-file reaction for $\kappa = 1.27 \times 10^{-5}$ ($\Phi = 2.77$). x denotes the distance from the middle of the file and $L = Nl$ its length.

$$\Phi = \frac{L}{2}\sqrt{\frac{k}{D}}, \tag{16}$$

leading to the effectiveness factor

$$\eta = \frac{\tanh \Phi}{\Phi} \tag{17}$$

The Thiele modulus may be represented in an alternative way by introducing the intracrystalline mean lifetime τ_{intra} of the molecules within the catalyst particles as defined by the first statistical moment of the tracer exchange curve (*43*)

$$\tau_{intra} = M_1 = \int_{t=0}^{\infty} \left[1 - \frac{\Theta(t)}{\Theta(\infty)}\right] dt. \tag{18}$$

In the case of a parallel-sided slab of thickness L, one has (*43*)

$$\tau_{intra} = \frac{L^2}{12D}. \tag{19}$$

Inserting this expression into Eq. (16) yields for the Thiele modulus

$$\Phi = \sqrt{3k\tau_{intra}}. \tag{20}$$

With this more general notation, the application of the Thiele modulus is evidently not only restricted to transport patterns following ordinary diffusion.

In Fig. 10b the various values of the effectiveness factor given in Fig. 10a are represented as a function of the generalized Thiele modulus, defined in this manner. The values of the molecular mean lifetime τ_{intra} have been determined on the basis of Eq. (18) from the simulated tracer exchange curves. For a given site occupancy the effectiveness factor, as for ordinary diffusion, is found to be a function of the Thiele modulus, which approaches the pattern of ordinary diffusion (Eq. (17)) with decreasing concentration.

Over the range considered in our simulations ($0.2 < \Theta < 0.8$) the intracrystalline mean lifetimes as calculated on the basis of Eq. (18) from the tracer exchange curves were found to be represented by the expression

$$\tau_{intra} = \frac{1}{350}\frac{\Theta^{3/2}}{1-\Theta} N^4 \tau \tag{21}$$

within a scattering width of 10%. For identical intrinsic activities, according to Eq. (20) the ratio of the Thiele moduli for the single-

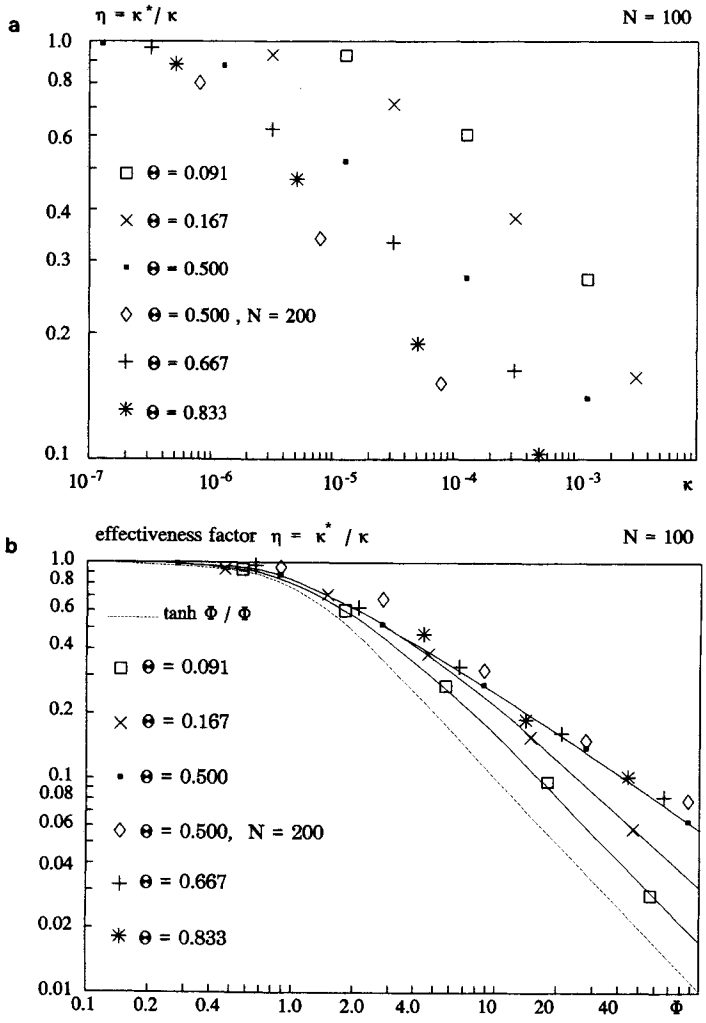

FIG. 10. Effectiveness factor $\eta = \kappa^*/\kappa$ of single-file reaction plotted in dependence of the intrinsic reaction rate (a) and the generalized Thiele modulus (b). The symbols in both representations refer to the same simulation conditions.

file and ordinary diffusion is given by the square root ratio of the mean life times τ_{intra}. Hence, by combining Eqs. (19) and (21), one obtains

$$\frac{\Phi_{\text{s.f.}}}{\Phi_{\text{ord.diff}}} = \sqrt{\frac{3}{175}\frac{\Theta^{3/2}}{1-\Theta}}N. \qquad (22)$$

With molecular mean jump lengths of l = 5 Å and particle diameters $L = Nl$ of the order of 1 μm, typical values of N should be of the order of 2000, leading to an enhancement of the Thiele modulus for the transition from ordinary to single-file diffusion over two to three orders of magnitude. These high values suggest that the catalytic reactions observed with single-file systems (*44–46*) are strongly transport-controlled and are most likely to occur in the vicinity of the orifices of the zeolite channels.

CONCLUSIONS

(i) In contrast to adsorption and desorption kinetics, which remain unchanged by

the transition from normal to single-file diffusion, tracer exchange and chemical reaction are dramatically retarded in single-file systems.

(ii) A key quantity for the description of single-file systems is the molecular mean square displacement. Monte Carlo simulations confirm the dependence on both the observation time ($\propto t^{1/2}$) and the sorbate concentration ($\propto (1 - \Theta)/\Theta$) of the long-time approaches predicted by theory.

(iii) Molecular confinement within single-file systems leads to an accumulation of the reaction products within the adsorbent, which is much more pronounced than in the case of ordinary diffusion.

(iv) Representing the Thiele modulus in terms of the molecular intracrystalline mean lifetimes allows its application to both ordinary and single-file diffusion. On the basis of the Thiele concept generalized in this way, a comparison of the influence of transport limitation in the cases of ordinary and single-file diffusion becomes possible.

(v) The single-file systems exhibit no peculiarities in their equilibrium properties.

APPENDIX

Derivation of the Long-Time Limit of the Molecular Mean Square Displacement in Single-File Systems

The elementary step of molecular migration along a single file may be interpreted as an exchange process between an occupied and a vacant site. Let us characterize the positions of the individual vacant sites at time t with respect to an arbitrarily chosen molecule by a set of integers $m_i(t)$, so that $m_i(t)l$ denotes the distances of the vacancies from the considered molecule. Since the displacement $r(t)$ of this molecule at time t results as the net effect of exchanges between this molecule and all vacancies, which have "migrated" from one side of this molecule to the other, we have

$$r(t) = l \sum_i [\vartheta(m_i(t)) - \vartheta(m_i(0))] \quad \text{(A1)}$$

with

$$\vartheta(m) = \begin{cases} +\frac{1}{2} & \text{for } m > 0 \\ -\frac{1}{2} & \text{for } m < 0. \end{cases} \quad \text{(A2)}$$

Thus, for the mean square displacement one obtains

$$\langle r^2(t)\rangle = l^2 \sum_{i,j} \langle [\vartheta(m_i(t)) - \vartheta(m_i(0))] \times [\vartheta(m_j(t)) - \vartheta(m_j(0))]\rangle. \quad \text{(A3)}$$

Since the positions of the individual vacancies are independent of each other, the sum over $i \neq j$ on the right-hand side of Eq. (A3) vanishes so that Eq. (A3) reduces to

$$\langle r^2(t)\rangle = l^2 \sum_i \langle [\vartheta(m_i(t)) - \vartheta(m_i(0))]^2\rangle. \quad \text{(A4)}$$

The sum on the right-hand side of Eq. (A4) represents the number of vacancies that has crossed the considered molecule either from left to right or from right to left. Adopting a treatment well known from PFG NMR (*26, 27*) and neutron scattering (*47*) the same quantity may be expressed in an alternative way by introducing the a priori probability $p_a(m)$ to find a vacancy at the m^{th} position, and the conditional probability $P_c(m, m', t)$ that a vacancy, initially at position m, will have migrated to m' at time t. This leads to

$$\langle r^2(t)\rangle = l^2 \sum_{m>0, m'<0} [p_a(m)P_c(m, m', t) + p_a(m')P_c(m', m, t)] \quad \text{(A5)}$$

The a priori probability of finding a vacancy is evidently equal to $(1 - \Theta)$. Considering sufficiently large time intervals, the sum may be replaced by an integral and one finally obtains

$$\langle r^2(t)\rangle = l^2(1 - \Theta) \int_{m=0}^{\infty} \int_{m'=-\infty}^{0} [P_c(m, m', t) + P_c(m', m, t)]\, dm\, dm'. \quad \text{(A6)}$$

For further computation it is convenient to differentiate both sides of Eq. (A6) with respect to time:

$$\frac{d}{dt}\langle r^2(t)\rangle$$

$$= l^2(1-\Theta)\int_{m=0}^{\infty}\int_{m'=-\infty}^{0}\left[\frac{\partial}{\partial t}P_c(m, m', t) + \frac{\partial}{\partial t}P_c(m', m, t)\right] dm\, dm'. \quad \text{(A7)}$$

The time derivatives of the conditional probabilities $P_c(m, m', t)$ are given by Fick's second law describing the propagation of the individual vacancies:

$$\frac{\partial P_c}{\partial t} = D_v\frac{\partial^2 P_c}{\partial (ml)^2} = \frac{D_v}{l^2}\frac{\partial^2 P_c}{\partial m^2}. \quad \text{(A8)}$$

Considering an isolated vacancy within a single file, the diffusivity D_v of this vacancy is evidently given by Eq. (2). For calculating the vacancy diffusivity under the influence of other vacancies we consider the mean square displacement of a certain vacancy during a time interval t. As soon as the selected vacancy is in contact with other vacancies, it cannot be distinguished from these others. This is equivalent with the understanding that the transfer rate of a given vacancy over other vacant sites is infinitely large. Thus, under the influence of other vacancies, the mean square displacement $\langle r^2(t)\rangle$ of a given vacancy,

$$\langle r^2_{\text{isol.}}(t)\rangle = 2Dt, \quad \text{(A9)}$$

if there were no other vacancies, would obey the relation

$$\Theta^2\langle r^2(t)\rangle = \langle r^2_{\text{isol.}}(t)\rangle. \quad \text{(A10)}$$

Combining Eqs. (A9) and (A10), the comparison with Einstein's relation (Eq. (1)) finally yields for the vacancy diffusivity

$$D_v = \frac{D}{\Theta^2} = \frac{l^2}{2\tau\Theta^2}. \quad \text{(A11)}$$

Since

$$\frac{\partial P_c}{\partial m} = -\frac{\partial P_c}{\partial m'}, \quad \text{(A12)}$$

Equation (A8) may be written in the form

$$\frac{\partial P_c}{\partial t} = -\frac{D_v}{l^2}\frac{\partial^2 P_c}{\partial m \partial m'}, \quad \text{(A13)}$$

which allows a straightforward solution of the integral of Eq. (A7), leading to

$$\frac{d}{dt}\langle r^2(t)\rangle = \frac{1-\Theta}{\Theta^2}\frac{l^2}{\tau}P_c(0, 0, t). \quad \text{(A14)}$$

$P_c(m, m', t)$ is the solution of Eq. (A8) for the initial condition

$$P_c(m, m', 0) = \delta(m - m') \quad \text{(A15)}$$

and is given by the standard diffusion expression

$$P_c(m, m', t) = \sqrt{\frac{\Theta^2\tau}{2\pi t}}\, e^{-((m-m')^2\Theta^2\tau/2t)}. \quad \text{(A16)}$$

Inserting this result into Eq. (A14) and integrating finally leads to Eq. (3)

$$\langle r^2(t)\rangle = l^2\frac{1-\Theta}{\Theta}\sqrt{\frac{2}{\pi}}\sqrt{\frac{t}{\tau}}.$$

Nomenclature

Arabic

D	self-diffusivity
D_v	vacancy self-diffusivity
E	adsorption energy
F	single-file mobility factor
F_0	concentration-corrected single-file mobility factor
K	Henry constant
k	intrinsic reactivity
k^*	effective reactivity
k_b	Boltzmann constant
L	file length ($= Nl$)
l	step length
M_1	first statistical moment
m_i	set of integers, characterizing the positions of vacant sites
N	number of sites per file
n	number of simulation steps
P	escape probability
$P_c(m, m', t)$	conditional probability that a molecule, initially at position m, will have migrated to m' at time t

p	pressure
$p_a(m)$	a priori probability of finding a vacancy at site $m(= 1 - \Theta)$
q	encounter rate
r	displacement
T	temperature
t	time
x	space coordinate
z	number of molecules per file
Greek	
η	effectiveness factor
Θ	site occupancy
$\vartheta(m)$	function defined by Eq. (A2)
κ	reaction rate
κ^*	effective reaction rate
τ	mean time between succeeding jump attempts
τ_{intra}	intracrystalline mean life time
Φ	Thiele modulus

ACKNOWLEDGMENTS

Both the group in Leipzig and the group in Stuttgart gratefully acknowledge financial support by the German Science Foundation (Deutsche Forschungsgemeinschaft). S. Ernst and J. Weitkamp moreover acknowledge funding by Fonds der Chemischen Industrie and Max Buchner-Forschungsstiftung.

REFERENCES

1. Flank, W. H., and Whyte, T. E., Eds., "Perspectives in Molecular Sieve Science," ACS Symposium Series 368. American Chemical Society, Washington, DC, 1988.
2. Karge, H. G., and Weitkamp, J., Eds., "Zeolites as Catalysts, Sorbents and Detergent Builders—Applications and Innovations." Elsevier, Amsterdam, 1989.
3. Jacobs, P. A., and van Santen, R. A., Eds., "Zeolites: Facts, Figures, Future." Elsevier, Amsterdam, 1989.
4. Öhlmann, G., Pfeifer, H., and Fricke, G., Eds., "Catalysis and Adsorption by Zeolites." Elsevier, Amsterdam, 1991.
5. Hodgkin, A. C., and Keynes, R. D., *J. Physiol. (London)* **128,** 61 (1955).
6. Rickert, H., *Z. Phys. Chem. N.F.* **43,** 129 (1964).
7. Riekert, L., *in* "Advances in Catalysis" (D. D. Eley, H. Pines, and P. B. Weisz, Eds.), Vol. 21, p. 281. Academic Press, New York, 1970.
8. Fedders, P. A., *Phys. Rev. B* **17,** 40 (1978).
9. Fedders, P. A., and Sankey, O. F., *Phys. Rev. B* **15,** 3580 (1977); Sankey, O. F., and Fedders, P. A., *Phys. Rev. B* **15,** 3586 (1977).
10. de Gennes, P. G., *J. Chem. Phys.* **55,** 572 (1971).
11. Kärger, J., Pfeifer, H., and Vojta, G., *Phys. Rev. A* **37,** 4514 (1988).
12. Manning, J. R., "Diffusion Kinetics for Atoms in Crystals." van Nostrand, Princeton, NJ, 1968.
13. Havlin, S., and Ben-Avraham, D., *Adv. Phys.* **36,** 695 (1987).
14. Heink, W., Kärger, J., Pfeifer, H., and Stallmach, F., *J. Am. Chem. Soc.* **112,** 2175 (1990).
15. Ruthven, D. M., *Can. J. Chem.* **52,** 3523 (1974).
16. Theodorou, D. N., and Wei, J., *J. Catal.* **83,** 205 (1983).
17. Germanus, A., Thesis, University of Leipzig, 1986.
18. Förste, C., Germanus, A., Kärger, J., Pfeifer, H., Caro, J., Pilz, W., and Zikánová, A., *J. Chem. Soc. Faraday Trans. 1* **83,** 2301 (1987).
19. Aust, E., Dahlke, K., and Emig, G., *J. Catal.* **115,** 86 (1986).
20. Pitale, K. K., and Rajadhyaksha, R. A., *Curr. Sci.* **57,** 172 (1988).
21. Palekar, M. G., and Rajadhyaksha, R. A., *Chem. Eng. Sci.* **40,** 1085 (1985).
22. Rajadhyaksha, R. A., Pitale, K. K., and Tambe, S. S., *Chem. Eng. Sci.* **45,** 1935 (1990).
23. Kärger, J., and Ruthven, D. M., "Diffusion in Zeolites," Wiley, New York, 1992.
24. Garcia, S. F., and Weisz, P. B., *J. Catal.* **121,** 294 (1990).
25. Richards, P. M., *Phys. Rev. B* **16,** 1393 (1977).
26. Kärger, J., and Pfeifer, H., *Zeolites* **7,** 90 (1987).
27. Kärger, J., Pfeifer, H., and Heink, W., *Adv. Magn. Res.* **12,** 1 (1988).
28. Kärger, J., and Spindler, H., *J. Am. Chem. Soc.* **113,** 7571 (1991).
29. Hong, U., Kärger, J., Pfeifer, H., Müller, U., and Unger, K. K., *Z. Phys. Chem.* **173,** 225 (1991).
30. June, R. L., Bell, A. T., and Theodorou, D. N., *J. Phys. Chem.* **94,** 8232 (1990).
31. Demontis, P., Fois, E. S., and Quartieri, S., *J. Phys. Chem.* **94,** 4329 (1990).
32. Jobic, H., Beé, M., and Kearley, G. J., *Zeolites* **9,** 312 (1989).
33. Ruthven, D. M., "Principles of Adsorption and Adsorption Processes," Wiley, New York, 1983.
34. Petzold, M., Diploma thesis, University of Leipzig, Department of Physics, 1991.
35. Kärger, J., *Langmuir* **4,** 1289 (1988).
36. Kärger, J., *AIChE J.* **28,** 417 (1982).
37. Pfeifer, H., Freude, D., and Kärger, J., *in* "Zeolites as Catalysts, Sorbents and Detergent Builders—Applications and Innovations" (H. G. Karge and J. Weitkamp, Eds.), p. 89. Elsevier, Amsterdam, 1989.
38. Caro, J., Bülow, M., Derewinski, M., Haber, J., Hunger, M., Kärger, J., Pfeifer, H., Storek, W., and Zibrowius, B., *J. Catal.* **124,** 367 (1990).
39. Qureshi, W. R., and Wei, J., *J. Catal.* **126,** 126 and 147 (1990).

40. Tsikoyiannis, J. G., and Wei, J., *Chem. Eng. Sci.* **46,** 233 and 255 (1991).
41. Förste, C., Kärger, J., and Pfeifer, H., *in* "Zeolites: Facts, Figures, Future" (P. A. Jacobs and R. A. van Santen, Eds.), p. 907. Elsevier, Amsterdam, 1989.
42. Karge, H. G., and Niessen, W., *Catal. Today* **8,** 451 (1991).
43. Barrer, R. M., "Zeolites and Clay Minerals as Sorbents and Molecular Sieves." Academic Press, London, 1978.
44. Kumar, R., Ernst, S., Kokotailo, G. T., and Weitkamp, J., *in* "Innovation in Zeolite Materials Science" (P. J. Grobet, W. J. Mortier, E. F. Vansant, and G. Schulz-Ekloff, Eds.), pp. 451–459. Elsevier, Amsterdam/Oxford/New York/Tokyo, 1988.
45. Ernst, S., Weitkamp, J., Martens, J. A., and Jacobs, P. A., *Appl. Catal.* **48,** 137 (1989).
46. Kumar, R., and Ratnasamy, P., *J. Catal.* **116,** 440 (1989).
47. van Hove, L., *Phys. Rev.* **95,** 249 (1954).